Invited Paper

Terahertz polarizer of femtosecond pulse laser ablated two-dimensional $Ti_3C_2T_x$ MXene thin-film

Weimin Huang [1], Zihan Zhao [1], Genhao Gong [1], La Li [2], and Zhenyu Zhao [1*]
[1] Department of Physics, Shanghai Normal University, Shanghai 200234, China
[2] Institute of Semiconductors, Chinese Academy of Sciences, Beijing 100083, China
[*1] Email: zyzhao@shnu.edu.cn

(Received January 2023)

Abstract: We demonstrate flexible terahertz polarizer of two-dimensional materials MXene via femtosecond pulse laser ablation techniques. The femtosecond pulse laser causes the stripe-lines on the 30 μm thick thin-film of $Ti_3C_2T_x$ MXene-on-polyimide. One type of polarizer is of 2.5 μm stripe-lines at 1 μm interval distance, and another type of polarizer is of 2.7 μm stripe-lines at 1.55 μm interval distance. Both of these polarizers exhibit electric field extinction ratios in excess of 5 *dB*. Our works manisfest a cost-effective approach to achieve large area terahertz polarisers rapidly.

Keywords: MXene, Electromagnetic shielding, Terahertz polarizer, Laser ablation

Doi:

1. Introduction

Terahertz (1 THz=10^{12} Hz) band is an upcoming frequency region for wireless communication networks, which allows high-speed wireless extension of the optical fibers to beyond 5G and enable more effective data transfer ratio up to Tb/s [1, 2]. Due to the rising number of devices working in terahertz band, effective shielding of electromagnetic interference (EMI) is required owing to electromagnetic compatibility in between different devices [3]. Traditionally, metallic Faraday cage exhibits high shielding effect in a wide range of electromagnetic spectrum. However, the metal grid will add the weight for the whole terahertz system, and has the risk of short-circuit in a compact terahertz device. It is favorable to engineer EMI shielding materials with small thickness, high shielding effectiveness (SE), good flexibility and stability [4]. Alternatively, a two-dimensional (2D) material for terahertz EMI shielding application will be a better approach. 2D materials, normally described as monolayer atomic or molecular sheet have become a fascinating research topic since graphene was successfully exfoliated for the first time [5]. In contrast to their bulk counterpart, 2D materials have ultra-high specific surface area and possess energy band structures that can be sensitive to external radiation perturbations. Owing to such a figure of merits, 2D materials are recognized as the device of interface [6]. Research on 2D materials not only contribute to the deeper understanding of their own intrinsic physical properties, but also become a great platform for the potential applications in the fields of

electronics and optoelectronics [6-10]. To date, 2D transition metal carbides, carbon-nitrides, and nitrides called MXene has attracted huge research attention due to their outstanding EMI performance [11]. MXene exhibits very large absorption in broadband spectrum from visible light to terahertz frequency range [11-16]. Currently, more than 20 members of the MXene family have been synthesized, and dozens more are predicted, making it one of the fastest growing 2D material families. Among the family of MXene, $Ti_3C_2T_x$ MXene was produced using a HF-containing etchant such as ammonium bifluoride (NH_4HF_2) salt or HF through addition of lithium fluoride (LiF) salt to hydrochloric acid (HCl) [17]. The later significantly simplifies the synthesis method and improves the electronic properties of MXene, facilitating its use for EMI shielding [12-17].

Normally, materials of high EMI shielding ratio is also available to be a polarizer as long as it become a microstructure of stripe-lines, just like the grid-polarizer [18]. MXene patterning can be conducted by using microcontact printing techniques or photolithography. Compared to the previous two methods, femtosecond pulse laser ablation becomes a cost-effective method to achieve microstructure devices. Especially, the scanning area of laser ablation is much larger than the mask-size of photolithography. Such a method has been successfully used in making microstructure terahertz devices [19-20]. As such, it is a potential solution that one can achieve microstructured MXene devices.

In our work, we successfully make MXene-based flexible terahertz polarisers using femtosecond pulse laser ablation. The femtosecond laser pulse irradiates two types of MXene synthesized by different chemical process. As such, the width and interval distance between stripe-lines are different. Both types of polarisers exhibit more than 5 *dB* electric field extinction ratios.

2. Experiments

The MXene polarizer device, consisting of a pattern of parallel lines, is made by first applying MXene drop coating to a polyimide substrate and then processing it by laser etching printing.

The synthesis of MXene in Sample A is different from that in Sample B. For convenience, the MXene in sample A is referred to as type A MXene and the MXene in sample B is referred to as type B MXene. The detailed fabrication process of both types of $Ti_3C_2T_x$ MXene thin films are illustrated in Fig.1 (a). For the MXene type A, 0.5 *g* of Ti_3AlC_2 MAX was added into LiF (12 *mL*) / HCl (9 *mL*) and stirred at room temperature for 24 *h*. The sediment is washed with DI water several times until the pH value reached neutral, then monolayer $Ti_3C_2T_x$ is obtained from the supernatant after centrifugation at 3500 *rpm* for 5 *min*. For the MXene type B, 1.5 *g* of Ti_3AlC_2 MAX phase is added into a mixture of deionized (DI) water (13.5 *mL*)/HCl(13.5 *mL*)/HF(3 *mL*), and stirred at room temperature for 24 *h*. The sediment is washed with DI water several times until the pH value reached neutral, which is then added into 15 *mL* DI water containing 1.5 *g* of

LiCl under vigorous stirring at room temperature for 12 *h*. The monolayer $Ti_3C_2T_x$ suspension is washed with DI water several times and collected by centrifugation at 3500 *rpm* for 5 *min*. The $Ti_3C_2T_x$ MXene thin-film is achieved by drop-cast process. Both type of $Ti_3C_2T_x$ MXene suspension with a concentration of 3 *g/L* is spread on 25 *μm* thick polyimide substrate (DUPONT™ KAPTON®) and dried at 350 *K* for 20 *min* under vacuum.

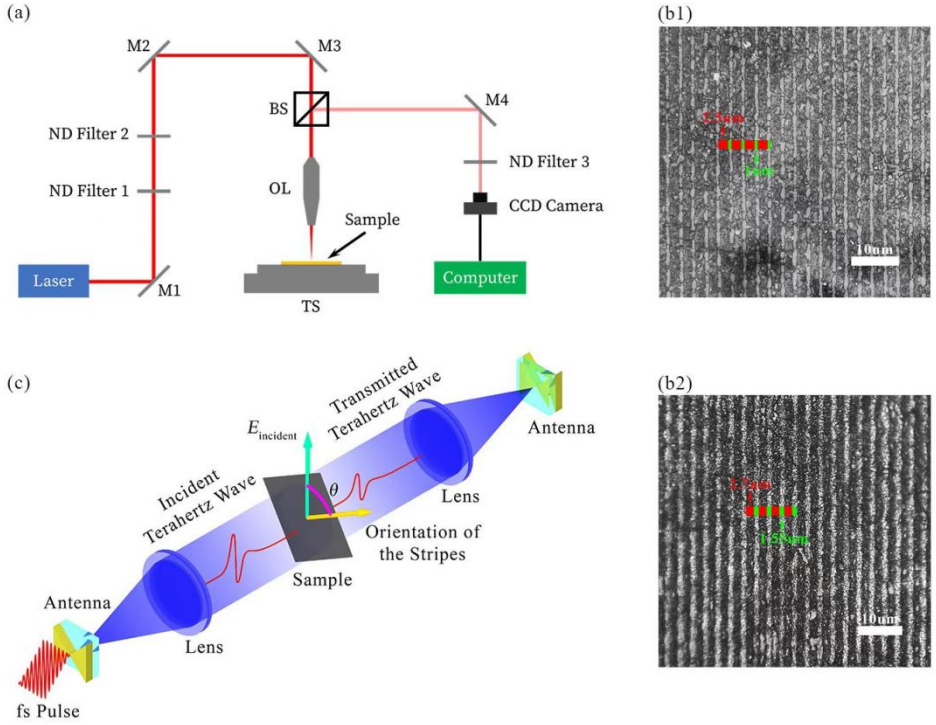

Fig. 1 (a) Schematic diagram of femtosecond laser ablation process. (b1) Microscopic image of Sample A. (b2) Microscopic image of Sample B. (c) Schematic diagram of THz-TDS.

After the synthetic processing of MXene, the sample is then subjected to laser engraving. First, the laser focal spot is gradually panned along the x-axis direction, so that the processed points are tangent to each other and connected into a straight line with a length of 1 *cm*, and then the ablation line is scanned row by row, with half of the laser focal spot spaced between the ablation rows, so that the scanned area reaches 1 *cm* × 1 *cm*. For sample A, the single pulse energy was set to 3.75 *μJ*, the pulse frequency was 2 *kHz*, the pulse width was about 9.18 *μm*, and the scanning speed was about 10 *mm/s*. For sample B, the single pulse energy was set to 4.5 *μJ*, the pulse frequency was 2 *kHz*, the pulse width was about 10.13 *μm*, and the scanning speed was about 10 *mm/s*. The samples were observed under a super depth-of-field microscope after processing, and the results are shown in Figure 1 (b1) and (b2). The MXene stripe width of sample A is about 2.5 *μm* and the inter-stripe interval is about 1 *μm*, while the width of the MXene stripe of sample B is about 2.7 *μm* and the inter-stripe interval is about 1.55 *μm*, after measurement under the microscope.

Fig. 1 (c) shows the diagram of terahertz time domain spectroscopy (THz-TDS) based on a fiber-coupled THz-TDS (TERA K15, Menlosystem GmbH) for performance evaluation. The incident terahertz pulse is incident normally onto the surface of the samples by a couple of TPX lens.

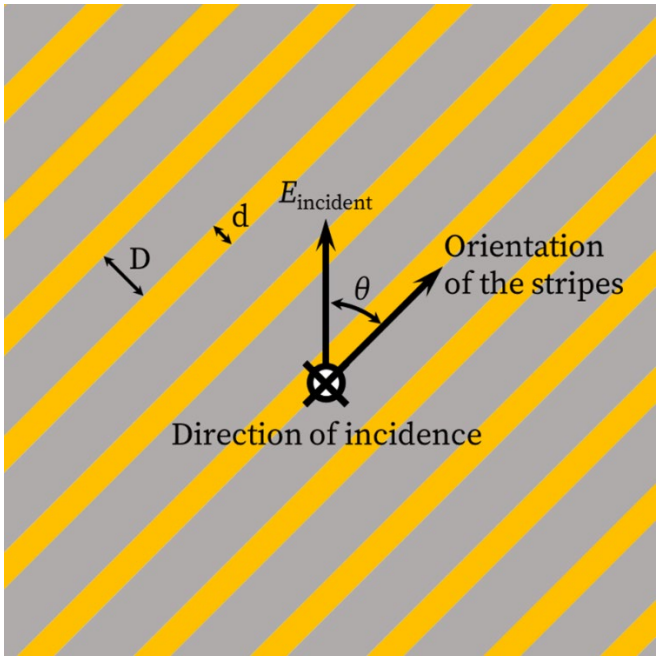

Fig. 2 Schematic diagram of the definition of θ angle. The gray part of the diagram shows the MXene stripes, the width of which is indicated by D. The yellow part shows the spacing between the stripes, which is the substrate polyimide, and the width of which is indicated by d.

The incident terahertz wave is polarized, as shown in Fig. 2, and its electric field vibration direction is at an angle of θ with the MXene stripe. The detected terahertz signals are read out into an integrated lock-in amplifier at the time constant of 100 *ms*. The terahertz response of the samples is measured in the range from 0.15 *THz* to 1.5 *THz*. The frequency resolution is about 10 *GHz*. All terahertz measurements are conducted in nitrogen atmosphere to avoid water absorption in air. A bare polyimide thin film identical to the sample substrate served as a reference.

3. Results and discussion

The terahertz pulse signals are shown in Fig. 3 (a) when only the polyimide substrate is present and when the stripes of the sample A and B are perpendicular to the polarization direction of the incident terahertz wave. After the Fourier transform, the time domain spectrum is converted to the frequency domain spectrum, and the results are shown in Fig. 3 (b).

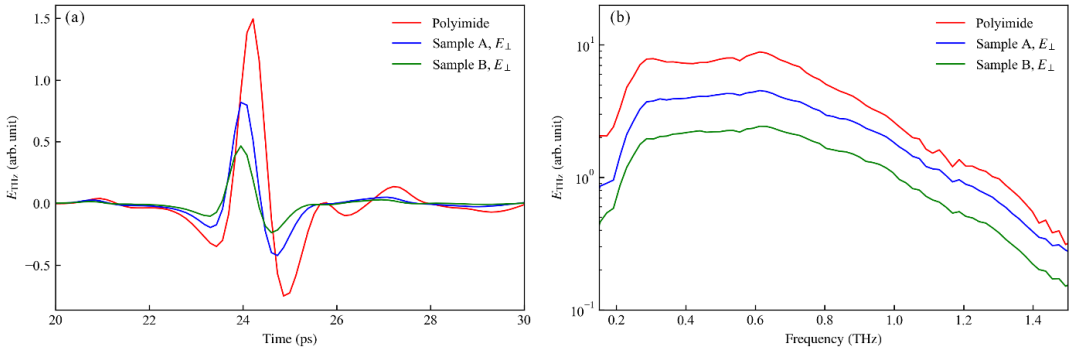

Fig. 3 (a) The transmission wave pulse waveforms of the substrate and the transmission pulse waveforms of the stripes of sample A and sample B perpendicular to the polarization direction of the incident terahertz wave. (b) Corresponding THz amplitude as a function of frequency.

The peak of the time domain spectrum allows us to observe the relationship between the intensity of the transmitted terahertz wave and the angle θ. Extinction ratio and insertion loss are important indicators to evaluate the performance of the sample. Through the frequency domain spectrum, we can find the extinction ratio and insertion loss of the two samples. The extinction ratio (ER) of the electric field intensity is defined as:

$$\mathrm{ER} = 10\log\left(\frac{E_\perp}{E_\parallel}\right), \tag{1}$$

The insertion loss (IL) of the electric field intensity is defined as:

$$\mathrm{IL} = -10\log\left(\frac{E_\perp}{E_{\mathrm{Polyimide}}}\right). \tag{2}$$

In the above two equations, $E_\parallel$ represents the transmitted electric field intensity when θ equals 0 degrees, $E_\perp$ represents the transmitted electric field intensity when θ equals 90 degrees, and $E_{\mathrm{Polyimide}}$ is the transmitted electric field intensity of the substrate polyimide.

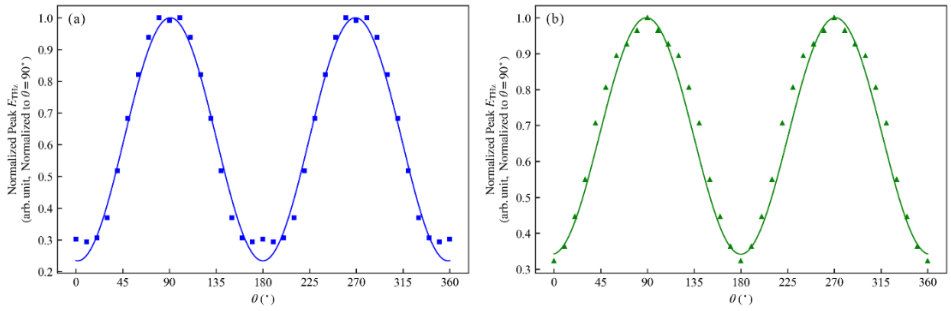

Fig. 4 Peak transmission pulse electric field intensities of (a) sample A and (b) sample B, normalized to its value for θ is 90 degrees. Symbols show experimental data, and lines are Malus's law fits. Note that, according to the symmetry principle, the experimental data were mirror-folded several times to cover 0 to 360 degrees.

A rotation of the sample by an angle θ about the normal produces a characteristic Malus's law dependence, as shown in Fig. 4. Fig. 4 (a) and Fig. 4 (b) show the peak transmission pulse electric field intensities of sample A and sample B at different θ angles with their fitting results, respectively. It should be noted that due to the existence of symmetry, we only did experiments with the θ ranging from 0 to 90 degrees and performed multiple mirror symmetries on the experimental data to achieve full angle coverage from 0 to 360 degrees. The resulting peak degrees of polarization, defined as below:

$$R = \frac{E_{\perp} - E_{\parallel}}{E_{\perp} + E_{\parallel}}. \tag{3}$$

To both samples, this value is approximately 50%.

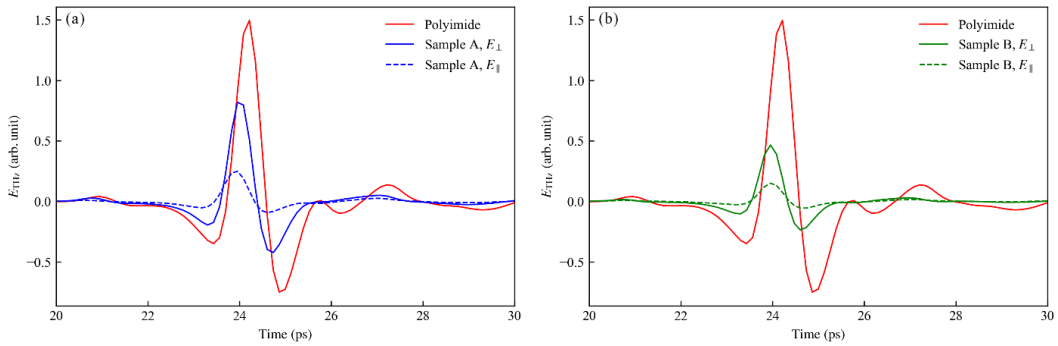

Fig. 5 The transmission pulse waveforms of the stripes of (a) sample A and (b) sample B perpendicular and parallel to the polarization direction of the incident terahertz wave. Reference THz pulses transmitted through the polyimide substrate are also shown.

The entire time-domain waveforms of the electric field for the two samples with the stripes perpendicular to the polarization direction of the incident terahertz wave and parallel to the polarization direction of the incident terahertz wave are shown in Fig. 5. The reference pulse through the substrate polyimide is also plotted in the figure. The data in Fig. 5 are Fourier transformed to obtain its frequency domain data, and it is used to calculate the extinction ratio as well as the insertion loss of the two samples, the results of which are shown in Fig. 6.

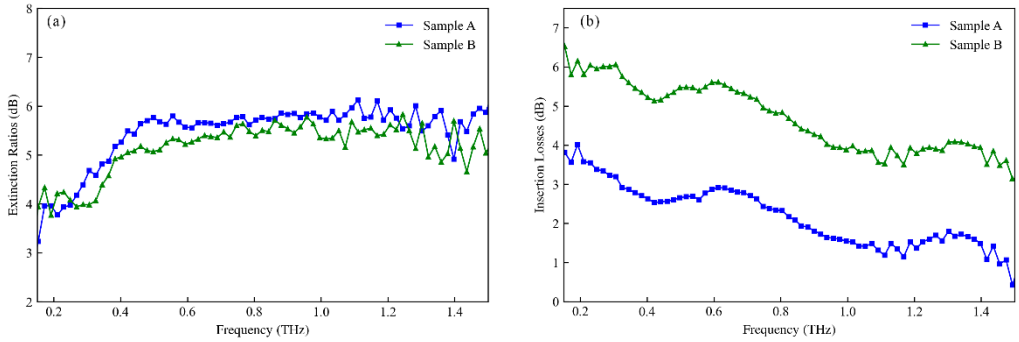

Fig. 6 (a) Electric field extinction ratios, and (b) insertion losses for the two samples.

The extinction ratios of both samples tend to increase with frequency in the 0.15 to 0.6 terahertz band, and then leveloff. Sample A has an average extinction ratio of 5.45 *dB* in the 0.15 to 1.5 terahertz band, while Sample B has a slightly weaker effect at 5.14 *dB*. As for the insertion loss, there is a decreasing trend with increasing frequency for both samples in the 0.15 to 1.5 terahertz band. Sample A has an average insertion loss of 2.19 *dB* in the 0.15 to 1.5 terahertz band, while Sample B has a much larger average insertion loss of 4.70 *dB*. Since the MXene dominates the EMI shielding properties, the difference of extinction ratio of sample A and B can be retrieved from the aspect ratio α of MXene stripe-lines. The aspect ratio is the width of MXene divided by the sum of width of MXene and interval distance. As such, the calculated α of sample A is 71.4%, and α of sample B is 63.5%. Obviously, the higher extinction ratio of sample A attributes to, the larger aspect ratio of MXene area is.

4. Conclusion

In conclusion, we show two samples of terahertz polarizers based on MXene coatings on polyimide substrates processed using the laser engraving method. The thickness of these two samples is about 30 *μm*, the stripe pattern is 2.5 and 2.7 *μm* wide, and the stripe spacing is 1 and 1.55 *μm* wide. They both have electric field intensity extinction ratios greater than 5 *dB* in the 0.15 to 1.5 terahertz band. In terms of insertion loss, the two samples do not perform particularly well, which suggests us to explore ways to reduce the insertion loss of the samples and maintain their extinction ratios to improve the sample performance in future work. Our work demonstrates the feasibility of using the laser engraving method to process MXene coatings to make terahertz polarizers, which can be used in the future to process low-cost terahertz polarization devices in short cycle and high volume for other MXene formulations to produce various new terahertz optoelectronic devices.

References

[1] T. Harter, C. Füllner, J. N. Kemal, et al. “Generalized Kramers-Kronig receiver for coherent THz communications”. *Nat. Photonics*, 14, 601–606 (2020).

[2] S. Dang, O. Amin, B. Shihada, et al. “What should 6G be?”. *Nat. Electronics*, 3, 20–29(2020).

[3] G. M. Kunkel. *Shielding of Electromagnetic Waves: Theory and Practice*. Berlin: Srpinger-Verlag (2020).

[4] X. C. Tong, *Advanced Materials and Design for Electromagnetic Interference Shielding*. Boca Raton: CRC Press (2008).

[5] K. S. Novoselov, A. K. Geim, S. V. Morozov, et al. “Electric field effect in atomically thin carbon films”. *Science*, 306, 666-669 (2004).

[6] X. Li , L. Tao , Z. Chen, et al. “Graphene and related two-dimensional materials: Structure-property relationships

for electronics and optoelectronics". *Appl. Phys. Rev.*, 4, 021306 (2017).

[7] Z. Sun, A. Martinez, and F. Wang. "Optical modulators with 2D layered materials". *Nat. Photonics,* 10, 227–238 (2016).

[8] A. Rodin, M. Trushin, A. Carvalho, et al. "Collective excitations in 2D materials". *Nat. Rev. Phys.*, 2, 524–537(2020).

[9] Y. Liu, X. Duan, H.-J. Shin, et al. "Promises and prospects of two-dimensional transistors". *Nature*, 591, 43–53(2021).

[10] L. Du, T. Hasan, A. Castellanos-Gomez, et al. "Engineering symmetry breaking in 2D layered materials". *Nat. Rev. Phys.*, 3, 193–206 (2021).

[11] A. Iqbal, F. Shahzad, K. Hantanasirisakul, et al. "Anomalous absorption of electromagnetic waves by 2D transition metal carbonitride $Ti_3C_NT_x$ (MXene)". *Science*, 369, 446-450 (2020).

[12] G. Choi, F. Shahzad, Y.-M. Bahk, et al. "Enhanced terahertz shielding of MXenes with nano-metamaterials". *Adv. Opt. Mater.*, 17, 1701076 (2018).

[13] W. Shui, J. Li, H. Wang, et al. "$Ti_3C_2T_x$ MXene sponge composite as broadband terahertz absorber". *Adv. Opt. Mater.*, 20, 2001120 (2020).

[14] J. Lipton, J. A. Röhr, V. Dang, et al. "Scalable, highly conductive, and micro-patternable MXene films for enhanced electromagnetic interference shielding". *Matter*, 3, 546–557 (2020).

[15] X. Jiang, A. V. Kuklin, A. Baev, et al. "Two-dimensional MXenes: From morphological to optical, electric, and magnetic properties and applications". *Phys. Rep.*, 848, 1–58 (2020).

[16] A. Iqbal, J. Kwon, M.-K. Kim, et al. "MXenes for electromagnetic interference shielding: Experimental and theoretical perspectives". *Mater. Today Advances*, 9, 100124 (2021).

[17] M. Alhabeb, K. Maleski, B. Anasori, et al. "Guidelines for synthesis and processing of two-dimensional titanium carbide ($Ti_3C_2T_x$ MXene)". *Chem. Mater.*, 29, 7633−7644 (2017).

[18] G. Li, K. Montazeri, M. K. Ismail, et al. "Terahertz polarizers based on 2D $Ti_3C_2T_z$ MXene: Spin cast from aqueous suspensions". *Adv. Photo. Res.* 1, 2000084 (2020).

[19] Z.-Y. Zhao, Z.-Q. Song, W.-Z. Shi, et al. "Optical absorption and photocurrent enhancement in semi-insulating gallium arsenide by femtosecond laser pulse surface microstructuring". *Opt. Express* 22, 11654-11659 (2014)

[20] J. Madéo, A. Margiolakis, Z.-Y. Zhao, et al. "Ultrafast properties of femtosecond-laser-ablated GaAs and its application to terahertz optoelectronics". *Opt. Lett.* 40, 3388-3391 (2015)